Anomalous L-Type Calcium Channels of Rat Spinal Motoneurons

Bruno Hivert, Siro Luvisetto, Anacleto Navangione, Angelita Tottene, and Daniela Pietrobon

From the Department of Biomedical Sciences and Consiglio Nationale delle Rícerche Center of Biomembranes, University of Padova, 35121 Padova, Italy

ABSTRACT Single channel patch-clamp recordings show that embryonic rat spinal motoneurons express anomalous L-type calcium channels, which reopen upon repolarization to resting potentials, displaying both short and long reopenings. The probability of reopening increases with increasing voltage of the preceding depolarization without any apparent correlation with inactivation during the depolarization. The probability of long with respect to short reopenings increases with increasing length of the depolarization, with little change in the total number of reopenings and in their delay. With less negative repolarization voltages, the delay increases, while the mean duration of both short and long reopenings decreases, remaining longer than that of the openings during the preceding depolarization. Open times decrease with increasing voltage in the range −60 to +40 mV. Closed times tend to increase at $V > 20$ mV. The open probability is low at all voltages and has an anomalous bell-shaped voltage dependence. We provide evidence that short and long reopenings of anomalous L-type channels correspond to two gating modes, whose relative probability depends on voltage. Positive voltages favor both the transition from a short-opening to a long-opening mode and the occupancy of a closed state outside the activation pathway within each mode from which the channel reopens upon repolarization. The voltage dependence of the probability of reopenings reflects the voltage dependence of the occupancy of these closed states, while the relative probability of long with respect to short reopenings reflects the voltage dependence of the equilibrium between modes. The anomalous gating persists after patch excision, and therefore our data rule out voltage-dependent block by diffusible ions as the basis for the anomalous gating and imply that a diffusible cytosolic factor is not necessary for voltage-dependent potentiation of anomalous L-type channels.

KEY WORDS: Ca^{2+} channel • dihydropyridine • gating • voltage-dependent potentiation

introduction

Among the different types of neuronal voltage-gated calcium channels, L-type channels play a specific role in regulating activity-dependent gene expression (Murphy et al., 1991; Bading et al., 1993; Deisseroth et al., 1998), neuronal survival and differentiation (Collins et al., 1991; Ghosh et al., 1994; Galli et al., 1995; Finkbeiner and Greenberg, 1996; Shitaka et al., 1996; Brosenitsch et al., 1998; Kirsch and Betz, 1998), and some forms of synaptic plasticity (Grover and Teyler, 1990; Aniksztejn and Ben-Ari, 1991; Johnston et al., 1992; Kullmann et al., 1992; Bolshakov and Siegelbaum, 1994).

Multiple functionally and structurally different neuronal L-type channels have been described (Snutch et al., 1991; Williams et al., 1992; Forti and Pietrobon, 1993; Kavalali and Plummer, 1994; Soldatov et al., 1995; Ferroni et al., 1996). In addition to classical cardiac-type channels, anomalous L-type channels, which reopen upon repolarization to resting potentials after a depolarization, have been reported in cerebellar, hippocampal, and sensory neurons (Fisher et al., 1990; Slesinger and Lansman, 1991, 1996; Forti and Pietrobon, 1993; Thibault et al., 1993; Kavalali and Plummer, 1994, 1996; Ferroni et al., 1996; Cloues et al., 1997). The probability of reopening of these L-type channels is voltage dependent, increasing with increasing voltage of the previous depolarization.

Different authors have proposed and supported different mechanisms accounting for voltage-dependent reopenings of L-type channels. Forti and Pietrobon (1993) have proposed that long reopenings of anomalous L-type channels are a manifestation of a voltage-dependent equilibrium between gating modes, whereby increasing voltage drives the channel from a short- to a long-opening mode (Pietrobon and Hess, 1990), and also increases the occupancy of a closed state outside the activation pathway, which is connected to the open state through a voltage-dependent transition within each mode. This additional closed state accounts for both the delay with which long openings occur upon repolarization of the membrane and the anomalous voltage dependence of the mean open/closed times and of the open probability, found by the same authors

Address correspondence to Daniela Pietrobon, Department of Biomedical Sciences, University of Padova, Viale Colombo 3, 35121 Padova, Italy. Fax: 39-049-8276049; E-mail: dani@civ.bio.unipd.it

(Forti and Pietrobon, 1993). Alternatively, reopenings have been interpreted as a manifestation of recovery from voltage- and/or current-dependent inactivation (Slesinger and Lansman, 1991; Thibault et al., 1993), resulting from voltage-dependent block of the channel pore by a positively charged cytoplasmic particle (Slesinger and Lansman, 1996). Kavalali and Plummer (1994, 1996) have proposed that reopenings reflect a particular form of voltage-dependent potentiation (LVP) in which the conditioning depolarization essentially reduces the voltage necessary to activate the channel. The different interpretations might reflect real differences in the L-type channels under study or simply derive from the emphasis of different aspects of the functional properties of essentially similar anomalous L-type channels. The data presented in this paper favor the second hypothesis.

As in most other neurons, the high-voltage activated whole-cell calcium current of embryonic and neonatal motoneurons can be dissected into four (L-, N-, P-, and R-type) pharmacological components (Mynlieff and Beam, 1992; Umemiya and Berger, 1994; Hivert et al., 1995; Magnelli et al., 1998). It is not known whether motoneurons express anomalous L-type channels. In the only single channel characterization of calcium channels in motoneurons (Umemiya and Berger, 1995), a classical L-type channel has been described.

Here we show that embryonic rat spinal motoneurons express L-type channels that reopen at negative repolarization voltages and display anomalous gating properties similar to those of anomalous L-type channels of cerebellar granule cells. We have investigated the mechanism giving rise to the anomalous gating in motoneurons. Our data are consistent with the model proposed by Forti and Pietrobon (1993). They are also consistent with reversible block of the open pore by a positively charged cytoplasmic particle, but exclude block by diffusible ions, and imply that a diffusible cytosolic factor is not necessary for voltage-dependent potentiation of anomalous L-type channels.

materials and methods

Cell Culture

Spinal motoneurons from embryonic day 15 (E15) Wistar rat embryos were grown in primary culture after purification by a two-step metrizamide-panning method according to the procedure of Camu et al. (1993). In brief, ventral spinal cords were dissociated after trypsin digestion, and centrifuged over 6.5% metrizamide (Serva) cushions to eliminate the four-plate cells, which are dense enough to sediment through the cushion. The large cells were further enriched by immunopanning on Petri dishes coated with the IgG-192 antibody specific for the p75 neurotrophin receptor, which is specifically expressed by motoneurons at this stage. The hybridoma was generously provided by Dr. C.E. Henderson (University Mediterrane, Marseille, France). Routinely, 90% of purified neurons express p75 immunoreactivity (Camu et al., 1993). The cells were plated on polyornithine- (Sigma Chemical Co.) and laminin- (GIBCO BRL) coated glass coverslips, and cultured in Dulbecco's modified Eagle medium (GIBCO BRL) supplemented with 17 mM glucose, 0.87 μM insulin, 0.99 mM putrescine, 0.93 μM sodium selenite, 1.32 μM transferrin, 0.19 μM progesterone, 0.51 μM triiodothyronine, 0.45 μM tiroxine, 1.32 μM BSA (all purchased from Sigma Chemical Co.), 2 mM glutamine, 100 IU/ml penicillin, and 100 μg/ml streptomycin (all purchased from GIBCO BRL). 12 h after plating, the culture medium was supplemented with 25% muscle-conditioned medium, obtained from myotube cultures of newborn rat. Experiments were performed on motoneurons kept in culture from 1 to 5 d.

Patch-Clamp Recordings and Data Analysis

Single channel patch-clamp recordings followed standard techniques (Hamill et al., 1981). Currents were recorded with a DAGAN 3900 patch-clamp amplifier, low-pass filtered at 1 kHz (−3 dB; eight-pole Bessel filter), sampled at 5 kHz and stored for later analysis on a PDP-11/73 computer. Experiments were performed at room temperature (21–25°C).

Linear leak and capacitative currents were digitally subtracted from all records used for analysis. Current amplitude histograms were obtained from the data directly, with bin width equal to our maximal resolution (323.6 points/pA). For display, each histogram was normalized to the value of the zero current peak. Open probability, P_o, was computed by measuring the average current in a given single channel current record and dividing it by the unitary single channel current. Open-channel current amplitudes were measured by manually fitting cursors to well-resolved channel openings. A channel opening or closure was detected when more than one sampling point crossed a discriminator line at 50% of the elementary current. Histograms of open and closed times were fitted with sums of decaying exponentials. The best fit was determined by maximum likelihood maximization (Colquhoun and Sigworth, 1983) and the best minimum number of exponential components was determined by the maximum likelihood ratio test (Rao, 1973). Log binning and fitting of the binned distributions were done as described by McManus et al. (1987) and Sigworth and Sine (1987). Openings occurring with a delay of more than one sampling point after repolarization of the membrane at −80 or −60 mV were considered as reopenings. In the measurement of the fraction of traces with reopenings, reopenings were detected using a discriminator line at 33% of the elementary current, to decrease the number of missed short reopenings. To calculate the fraction of traces with long and short reopenings, we used a discriminating open time value, calculated from the double exponential open time histogram as the open time that equalized the number of openings of the fast exponential component falsely assigned as long openings and the number of openings of the slow exponential component falsely assigned as short openings (Demo and Yellen, 1991). Reopenings of duration longer than this value were considered as long reopenings and those of shorter duration as short reopenings. The pipette solution contained (mM) 90 $BaCl_2$, 10 TEACl, 15 CsCl, 10 HEPES, pH 7.4 with TEAOH. The bath solution was (mM) 140 K-gluconate, 5 EGTA, 35 L-glucose, 10 HEPES, pH 7.4 with KOH. The high-potassium bath solution was used to zero the membrane potential outside the patch. The dihydropyridine agonist (+)-(S)-202-791 (gift from Dr. Hof, Sandoz Co., Basel, Switzerland) was added (1 μM) to the bath solution in most recordings. Liquid junction potential at the pipette tip was +12 mV (pipette positive), and this value should be subtracted to all voltages to obtain the correct values of membrane potentials in cell attached recordings (Neher, 1992).

results

Figs. 1 and 2 show that embryonic rat spinal motoneurons express L-type channels which reopen after repolarization of the membrane and display anomalous gating properties similar to those of anomalous L-type channels of cerebellar granule cells (Forti and Pietrobon, 1993). The single channel current recordings in Figures 1 and 2 were obtained from cell-attached membrane patches of rat spinal motoneurons in primary culture, which contained only one channel. The membrane was held at −80 mV and depolarized to four different voltages for 724 ms, every 4 seconds, in the presence of the dihydropyridine (DHP)[1] agonist (+)-(S)-202-791 in the bath in Figure 1 and in its absence in Figure 2. The representative current traces and the normalized current amplitude histograms from all traces with activity display the main unusual voltage-dependent properties of anomalous L-type channels.

The first unusual property is represented by the reopenings occurring with some delay after repolarization of the membrane at −80 mV, a voltage well below the threshold for channel activation. Some of these reopenings are quite long, much longer than the openings of the same channel during the preceding depolarization (compare Fig. 1, +30- and +40-mV traces). The second unusual property is represented by the voltage dependence of the open probability and of the open and closed times. The open probability (P_o) does not increase with voltage in the usual sigmoidal manner, but reaches a maximum at +20 mV, and then decreases with increasing voltage, remaining low in the entire voltage range (Fig. 3 C). In three single-channel patches, the maximal P_o at +20 mV in the presence of DHP agonist was 0.12 ± 0.02. In each patch, average open probabilities were obtained from the traces with activity, without including nulls, which were a minority at each voltage (0–7% at

[1]*Abbreviation used in this paper:* DHP, dihydropyridine.

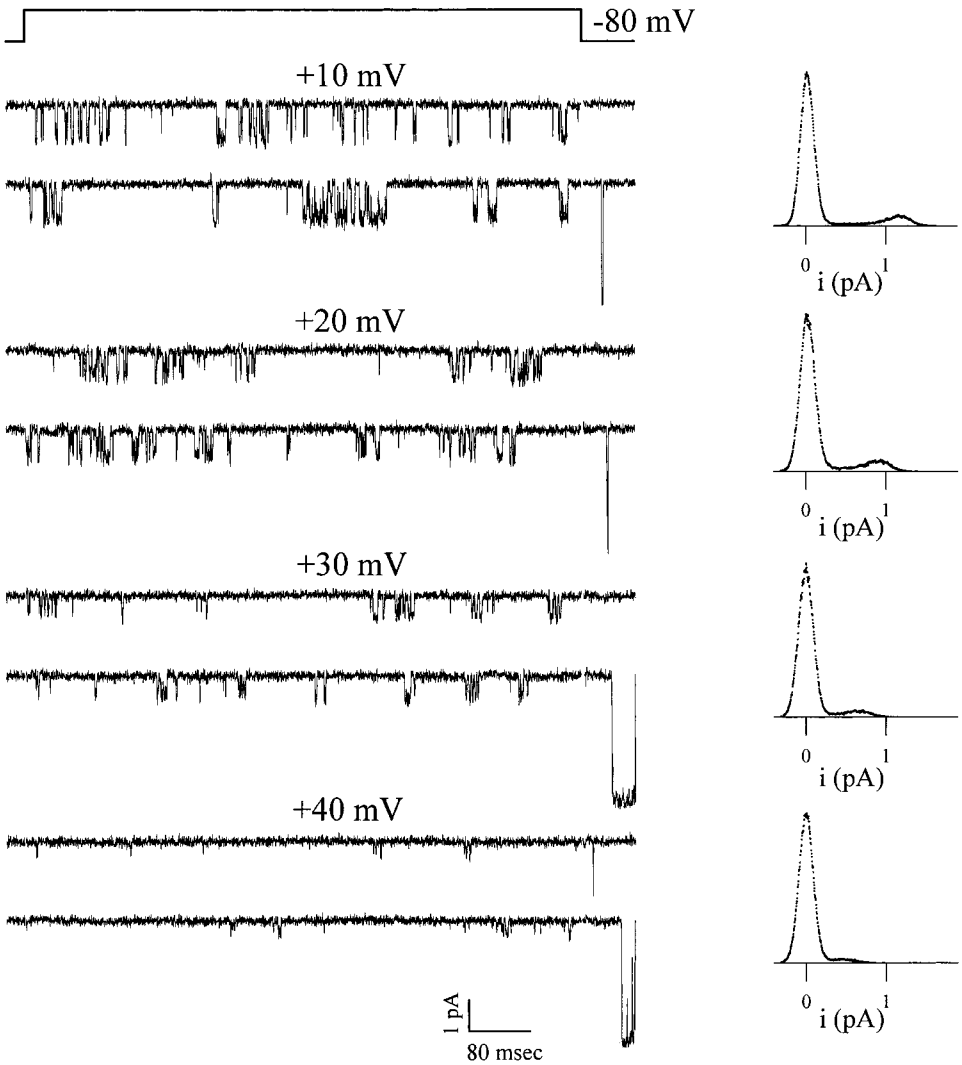

FIGURE 1. Single channel activity of the anomalous L-type Ca^{2+} channel of rat spinal motoneurons in the presence of DHP agonist. Cell-attached recordings with 90 mM Ba^{2+} as charge carrier from a patch containing a single L-type channel with anomalous gating, in the presence of 1 μM (+)-(S)-202-791 in the bath. Representative current traces at +10, +20, +30, and +40 mV are shown together with the normalized current amplitude histograms from all traces with activity at each voltage. Depolarizations were 724-ms long and were delivered every 4 s from holding potentials of −80 mV. Records were sampled and filtered at 5 and 1 kHz, respectively. Cell B58D.

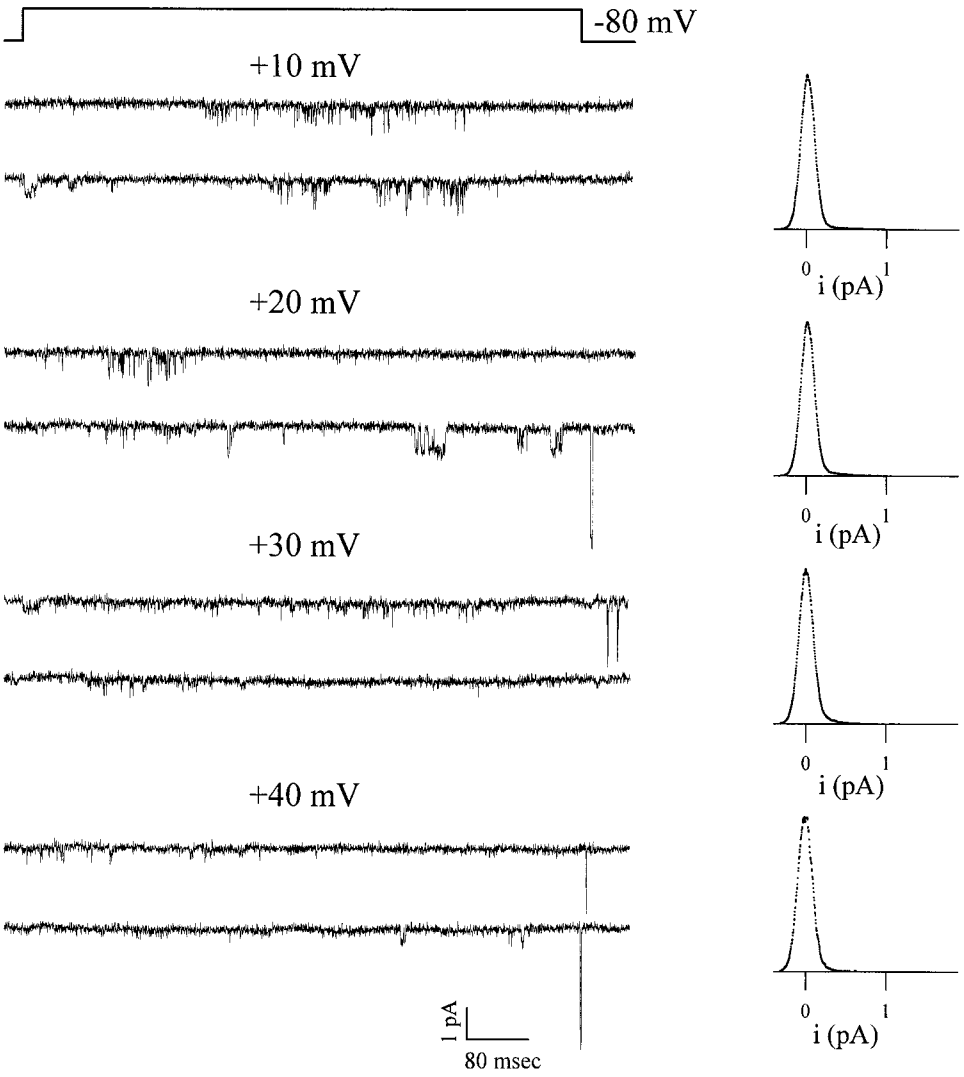

FIGURE 2. Single channel activity of the anomalous L-type Ca^{2+} channel of rat spinal motoneurons in the absence of DHP agonist. Cell-attached recordings from a patch containing a single L-type channel with anomalous gating. Experimental conditions and protocol as in Fig. 1, but without DHP agonist. Cell B05F. The patch also contained two T-type channels, as shown by the relatively long openings with small amplitude at the beginning of some of the traces. The second trace at +20 mV shows a transition from mode 1 to 2 of the anomalous L-type channel (see text).

+10 mV and 10–20% at +40 mV). In the absence of DHP agonist, the activity of anomalous L-type channels is characterized by brief, mostly unresolved and infrequent openings and by an extremely low open probability at all voltages: the maximal value of P_o was 0.024 in the single channel patch of Fig. 2. Kinetic analysis of the open and closed time histograms reveals that the low open probability and its anomalous voltage dependence are due to the anomalous voltage dependence of both open and closed time constants. As shown in Fig. 3, the time constants of the two exponential components best fitting open time histograms both decrease with increasing voltage, and the two larger time constants of the three exponential components best fitting closed time histograms decrease with voltage up to +20 mV, and then start to increase (see also Fig. 10 B). Interestingly, the contribution of the slow exponential component in the open time histograms increases with increasing voltage, with a symmetrical decrease of the fast component.

Thanks to these anomalous gating properties, anomalous L-type channels in the presence of DHP agonist could be easily distinguished from the other L- and non–L-type channels of rat spinal motoneurons. We have found that rat spinal motoneurons coexpress, together with the anomalous L-type channels characterized in this study, two additional DHP-sensitive channels, one similar to cardiac L-type channels and the other inactivating quite rapidly (Hivert and Pietrobon, 1995, 1997; and our unpublished observations). They can be distinguished from L-type channels with anomalous gating on the basis of their larger unitary current and conductance (24 vs. 20 pS), their larger mean open time and open probability at $V > +20$ mV (not decreasing with increasing voltage), and the complete absence of reopenings. Moreover, rat spinal motoneurons express several different DHP-insensitive calcium channels, including two channels sharing the same conductance of 20 pS but differing in inactivation and pharmacological properties (Hivert and Pietrobon, 1995; and our unpublished observations).

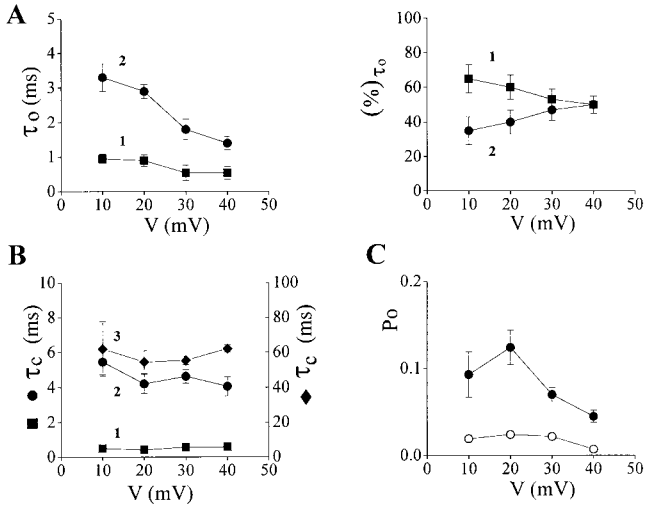

FIGURE 3. Anomalous voltage dependence of open probability and of open and closed times of anomalous L-type channels. Experimental conditions and protocol as in Fig. 1. Average values of open and closed time constants and open probabilities from three patches containing only one channel. (A, left) voltage dependence of the time constants, τ_{o1} and τ_{o2}, of the exponential components best fitting the open time distributions of single anomalous L-type channels. (Right) Average fractional areas of the two exponential components best fitting the open time distributions. (B) Voltage dependence of the time constants, τ_{c1}, τ_{c2}, and τ_{c3}, of the exponential components best fitting the closed time distributions. (C) Voltage dependence of the average open probability of single anomalous L-type channels in the presence of DHP agonist (●), and of the open probability in the absence of agonist from the patch in Fig. 2 (○). For each patch, P_o values were obtained by averaging the open probabilities measured in each sweep with activity, at a given voltage (n = 13–120). The best fit of open/closed time distributions was determined as described in MATERIALS AND METHODS. The best fit of the closed time distributions required a sum of three exponentials at each test potential. The best fit of the open time distributions required the sum of two exponentials at +10, +20, and +30 mV, while, at +40, one or two exponentials were equally likely.

In this study, we have investigated the mechanism giving rise to the unusual voltage-dependent properties of anomalous L-type channels of rat spinal motoneurons. To discriminate between different mechanisms, it was essential to be able to study the activity of a single anomalous channel during both the depolarization and repolarization periods. Since anomalous L-type channels represent only a small fraction of the different types of calcium channels with similar conductance expressed in motoneurons and patches with only one anomalous L-type channel were very rare, and since, in addition, the open probability of single anomalous L-type channels in the absence of DHP agonist is extremely low (Figs. 2 and 3 C), a property that they share with the more abundant inactivating L-type channel of 24 pS, it was necessary to prolong the openings of L-type channels with a DHP agonist to be sure that only one anomalous L-type channel was present in the patch. The comparison between Figs. 1 and 2 shows that the peculiar voltage-dependent properties of anomalous L-type channels above described are essentially similar with or without agonist, as previously shown in cerebellar granule cells (Forti and Pietrobon, 1993).

It has been proposed that reopenings of anomalous L-type channels reflect recovery from voltage- and/or current-dependent inactivation (Slesinger and Lansman, 1991, 1996; Thibault et al., 1993). If this interpretation is correct, then, in an experiment in which the membrane is depolarized at increasingly positive voltages, one should find a correlation between the extent of inactivation of single anomalous L-type channels during the depolarization and the fraction of traces with reopenings upon repolarization. Fig. 4 shows that such a correlation is absent. The ensemble average currents from a patch containing a single anomalous L-type channel in Fig. 4 A shows a lack of inactivation during long depolarizations at positive voltages (+10 to +40 mV) elicited from quite negative holding potentials (−80 mV). In the same voltage range, the fraction of traces with reopenings at −80 mV of the same channel increased as shown in Fig. 4 B (from 0 to 62%). Similar results were obtained for single anomalous L-type channels in cerebellar granule cells (Forti and Pietrobon, unpublished observations). Thus, the previously reported absence of inactivation of cerebellar anomalous L-type channels during depolarizations effective in inducing reopenings (Forti and Pietrobon, 1993) cannot be ascribed to the relatively depolarized holding potentials, as recently suggested (Slesinger and Lansman, 1996), but appears as a general distinctive property of anomalous L-type channels.

As already pointed out, after long depolarizations, both short and long reopenings at −80 mV could be observed. The existence of two clearly different open states, one short and the other long lasting, is even more evident if one analyzes the reopenings at −60 mV after a 400-ms long depolarization to +40 mV (Fig. 5, left). The recordings in Fig. 5 were obtained from a cell-attached patch containing only one anomalous L-type channel. The open time histogram of reopenings at −60 mV required two exponential components with time constants of 1.8 and 29 ms for best fit according to the maximum likelihood criterion. Strikingly, both open time constants were larger (1.6 ± 0.1 and 26 ± 3 ms, n = 5) than those measured for the anomalous L-type channel during the predepolarization at +40 mV (0.54 ± 0.19 and 1.4 ± 0.2 ms, n = 3; see Fig. 3).

A common feature of the different single L-type channels described so far is their voltage-dependent modal gating, whereby increasing voltage progressively drives the channels from a short-opening mode of activity (mode 1), prevailing at low voltages, to a long-

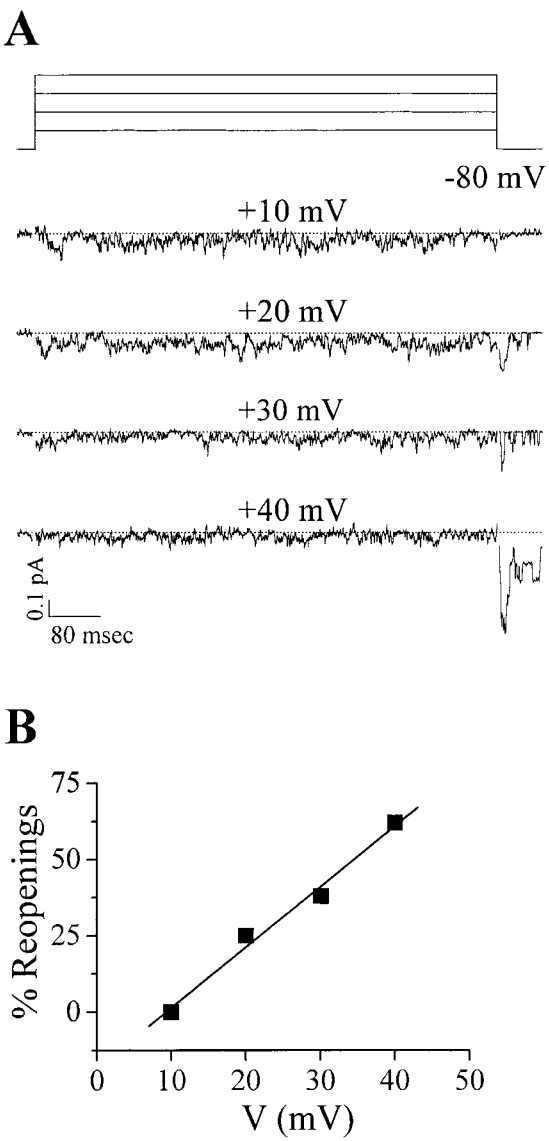

FIGURE 4. Lack of correlation between probability of reopening and inactivation of single anomalous L-type channels. (A) Ensemble average currents of a single anomalous L-type channel during 724-ms–long depolarizations at four different voltages and during repolarization at −80 mV, in the presence of 1 μM (+)-(S)-202-791 in the bath. The numbers of averaged sweeps were 42, 56, 45, and 40 at +10, +20, +30, and +40 mV, respectively. (B) Voltage dependence of the probability of reopening of the same single channel at −80 mV after 724 ms at different voltages, calculated as the fraction of sweeps with reopenings occurring during the 72 ms at −80 mV after depolarizations in which the channel was active (% Reopenings). Only openings at −80 mV occurring with a delay of at least two sampling points (400 μs) after repolarization, and with amplitude higher than 33% of the single channel current at −80 mV were considered. Ensemble average currents and probabilities of reopening were obtained after excision of a patch containing only one channel. As shown in Fig. 10, the anomalous gating persisted unaltered after patch excision. Cell B48L.

opening mode (mode 2) prevailing at high positive voltages (Pietrobon and Hess, 1990; Forti and Pietrobon, 1993; Kavalali and Plummer, 1996). Forti and Pietrobon (1993) proposed that the anomalous gating arises from the presence of a nonadsorbing closed state outside the activation pathway connected to the open state through a voltage-dependent transition within each mode, and used the simplified kinetic scheme of Fig. 6 to explain, at least qualitatively, the peculiar properties of cerebellar anomalous L-type channels. In this kinetic model, the individual open and closed states underlying the two modes within the two boxes are lumped together and connected by single voltage-dependent forward (k_f) and backward (k_b) rate constants. To account for the anomalous voltage dependence of both open and closed times (see Fig. 3), the open states within each mode (O, O*) are connected to a closed state outside the activation pathway (C_b, C^*_b), and the rate constants α, α^* for entry into the closed states C_b in mode 1 and C^*_b in mode 2 are assumed to increase with voltage, while the rate constants β, β^* for exit from these closed states are assumed to decrease with voltage. Although the kinetic scheme in Fig. 6 is likely an oversimplification, we will use it here as a useful conceptual framework for the analysis and discussion of our data on anomalous L-type channels of motoneurons.

A possible interpretation of the presence of both short and long reopenings at negative voltages is that they represent reopenings of the channel in either mode 1 (from C_b) or mode 2 (from C^*_b), respectively. If this interpretation is correct, then any intervention that changes the probability of finding the channel in mode 2 at the end of the depolarization should change the relative proportion of long with respect to short reopenings, owing to the change in the relative probability of finding the channel in C^*_b with respect to C_b when the membrane is repolarized. The probability of finding the channel in the long-opening mode at the end of the depolarization can be changed by either changing the length or the amplitude of the depolarization. One expects that if the depolarization is shortened the relative proportion of long with respect to short reopenings should decrease. Indeed, Fig. 5 shows that when the depolarization was shortened from 400 to 50 ms, most of the reopenings of the single anomalous channel in the patch became short. The long reopenings were too few to define the second slower component in the open time histogram of the reopenings. The histogram was best fitted by a single exponential with a time constant of 2 ms, quite similar to the time constant of the fast component best fitting the histogram of reopenings of the same channel after 400 ms.

In three single channel patches, long reopenings were on average 40 ± 1% of the total number of reopenings after a 400-ms long depolarization, and de-

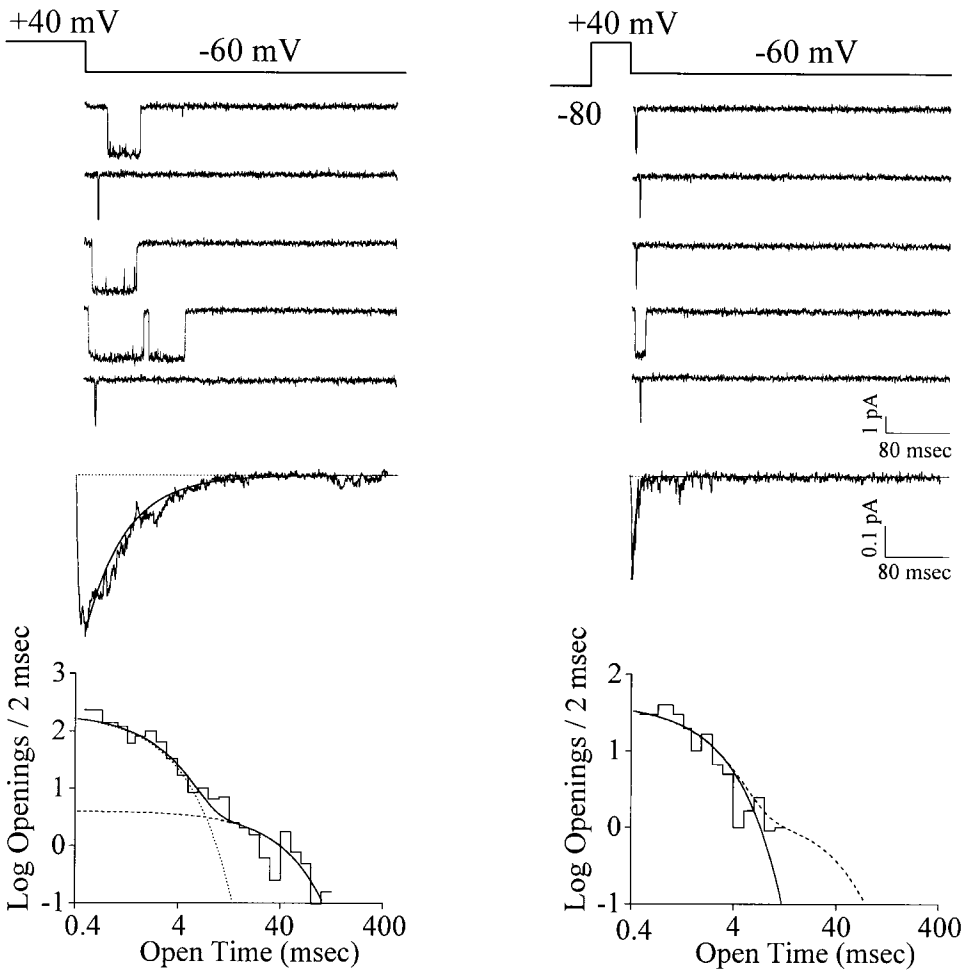

FIGURE 5. The relative proportion of short and long reopenings of anomalous L-type channels depends on the length of the depolarization. Cell-attached single channel recordings from a patch containing one anomalous L-type channel, in the presence of 1 μM (+)-(S)-202-791 in the bath. The voltage protocol consisted of the alternation of series of depolarizations to +40 mV lasting 400 ms, and series of depolarizations at the same voltage lasting 50 ms. After the depolarization, the voltage was repolarized to −60 mV. Holding potential was −80 mV. Representative traces showing reopenings at −60 mV after 400 (left) and 50 (right) ms at +40 mV are shown together with the corresponding open time distributions and the ensemble average currents at −60 mV. The dark solid line in the log–log plot of the open time distribution in the left panel is the best fitting sum of exponential components. As indicated by the maximum likelihood ratio test, the best fit of the open time histogram at −60 mV, after 400 ms at +40 mV (n = 99), required two exponential components (shown as dotted lines), with time constants of 1.8 and 29 ms and relative areas of 76 and 24%. According to the same criterion, the best fit of the open time distribution in the right panel (after 50 ms at +40 mV, n = 29) required only one component with time constant of 2 ms (dark solid line); shown for comparison, with a dotted line, is the sum of the two components best fitting the open time histogram in the left panel. The decay of the ensemble average currents at −60 mV was best fitted, according to the maximum likelihood criterion, with a single exponential with time constant of 50 ms (left, after 400 ms at +40 mV, n = 161 averaged sweeps) and 5.3 ms (right, after 50 ms at +40 mV, n = 58). The time constants of the monoexponential fit of the rising phase of the two average currents are 2.6 s (left) and 1.6 (right) ms. The ratio of the peak average currents at −60 mV after the short and long depolarization is 0.62. Cell M04G.

creased to 7 ± 4% of the total number of reopenings when the depolarization was shortened to 50 ms (Fig. 7 A). In one single channel patch, after shortening the depolarization at +40 mV from 400 to 50 ms, the voltage was increased to +150 mV keeping the duration constant at 50 ms. The long reopenings decreased from 38 to 12% of the total number of reopenings when the moderate depolarization was shortened, and increased again to 36% of the total number of reopenings when the amplitude of the short depolarization was increased. The relative increase of long with respect to short reopenings with increasing length and amplitude of the previous depolarization is consistent with the interpretation that short and long reopenings are associated with two different gating modes of the channel (mode 1 and mode 2) and with the existence of a voltage-dependent equilibrium between the gating modes whereby the probability of the long-opening mode (mode 2) increases with increasing voltage.

Consistent with this interpretation is also the finding that the probability of (long + short) reopenings, which depends on the probability of finding the channel in either C_b or C^*_b at the end of the depolarization, was not much affected by changing the length of the depolarization. In three single-channel patches, the probability of reopenings changed from 63 ± 7% after 400 ms at +40 mV to 50 ± 5% after 50 ms at the same voltage (Fig. 7 B), but the change was not statistically significant ($P < 0.2$). The model in Fig. 6 predicts that changing the length of the depolarization should produce mirror changes in the probabilities of long and short reopenings, with a consequent unchanged probability of (long + short) reopenings, if the intrinsic probabilities of C_b and C^*_b within the two individual

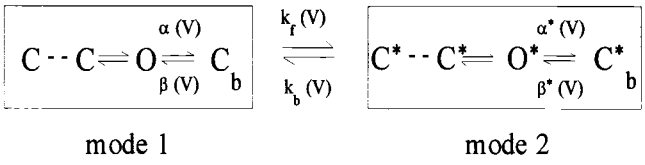

FIGURE 6. Simplified kinetic model for anomalous L-type channels proposed by Forti and Pietrobon (1993). The individual states within the boxes are lumped into modes of gating. Combining several individual states into one "mode" of gating is justifiable if transitions between states in a mode are much faster than transitions between modes. The rate constant of the transition O → C in mode 1 (the short-opening mode) is larger than the rate constant of the corresponding transition O* → C* in mode 2 (the long-opening mode). k_f and k_b, the rate constants of the transition between modes 1 and 2 are voltage dependent: k_f increases and k_b decreases with increasing voltage. As a result, the probability of mode 2 increases with increasing voltage. Also α, β and α*, β*, the rate constants of the transitions between the open states, O, O* and the closed states, C_b and C^*_b, within each mode, are voltage dependent: α, α* increase and β, β* decrease with increasing voltage. As a result the occupancy of the closed states, C_b and C^*_b increases with increasing voltage.

modes were identical and as long as the rate constants of the transitions to C_b and C^*_b were fast with respect to the duration of the depolarization.

As a consequence of the relative increase of long with respect to short reopenings with increasing length of the depolarization, the peak ensemble average current at −60 mV was larger and decayed more slowly after the longer depolarization (Fig. 5). In three single channel patches, the average time constant of decay of the ensemble current at −60 mV changed from 48 ± 1 ms after the long depolarization to 9.9 ± 5 ms after the short depolarization. On average, the ratio of the peak average currents at −60 mV after short and long predepolarizations was 0.49 ± 0.07. The ensemble averages at −60 mV after both long and short depolarizations showed a clear rising phase, which originates from the delay with which most reopenings occurred after the repolarization. The time constant of the rising phase after short depolarizations (1.5 ± 0.3 ms) was slightly smaller than that after long depolarizations (2.6 ± 0.5 ms), but the difference did not reach statistical significance ($P < 0.1$).

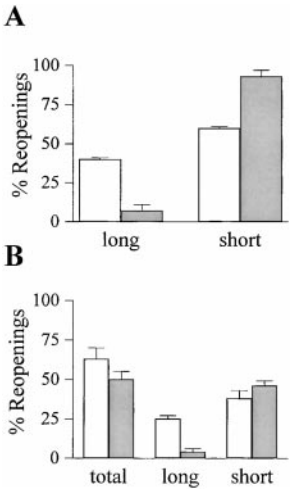

FIGURE 7. Relative increase of long with respect to short reopenings with increasing duration of the depolarization, with little change in the total number of reopenings. (A) Average relative fraction of long with respect to short reopenings at −60 mV after long (white bars) and brief (dark bars) depolarizations at +40 mV, obtained from three cell-attached patches with one anomalous L-type channel, using the same voltage protocol as in Fig. 5 (except that in one patch the duration of the short depolarization was 10 ms). % Reopenings represents the number of traces with short or long reopenings divided by the total number of traces with reopenings, calculated over a number of traces ranging from 113 to 172 for the long depolarization, and from 64 to 191 for the short depolarization. Long and short reopenings were separated using a discriminating open time value, calculated from the biexponential open time histogram (see MATERIALS AND METHODS). (B) Average probability of (short + long) reopenings and of either short or long reopenings at −60 mV after long (white bars) and brief (dark bars) depolarizations at +40 mV, obtained from the same three patches. % Reopenings represents either the number of sweeps with reopenings without distinction between short or long (total) divided by the total number of sweeps, or the number of sweeps with long or short reopenings divided by the total number of sweeps. The traces with unresolved reopenings of amplitude smaller than 1/3 of the single channel current at −60 mV were not counted.

Fig. 8 shows directly that long moderate depolarizations are able to drive anomalous L-type channels from a short- into a long-opening mode. The unitary current recordings in Fig. 8 A were obtained from a patch containing a single anomalous L-type channel, in an experiment in which after 400 ms at +30 mV the membrane was repolarized at −10 mV, a voltage just above the threshold for channel activation. Control depolarizations to −10 mV for 800 ms were alternated with the prepulse protocol. In the large majority of control depolarizations at −10 mV (in 98 of 102 traces with openings), the unitary activity was characterized by relatively short openings and long closings and a low open probability, as shown by the first five representative traces in Fig. 8 A (right). The last trace represents a small minority of depolarizations (4 of 102 active traces) in which the channel shifted to a different mode of activity, characterized by long-lasting bursts with longer openings and shorter closings and by a much larger open probability.

The representative traces and the ensemble average current of Fig. 8 A (left) show that a preceding depolarization to +30 mV for 400 ms increased the probability of observing the long opening mode, with a consequent potentiation of the average current at −10 mV. The fraction of active traces with the long opening mode increased from 4% in control depolarizations to 35% after 400 ms at +30 mV. These fractions were calculated using a discriminating open probability value of 0.1 to separate the traces with the long opening mode from those with activity similar to that in control. Fig. 8, B–D, shows that, while the open time histogram of all traces at −10 mV after the prepulse required two exponential components with time constants of 1.7 and 9.1 ms for best fit, the open time histogram of the traces with $P_o < 0.1$ could be best fitted by a single exponential with a time constant of 1.6 ms, similar to that of the fast component in the overall histogram and to

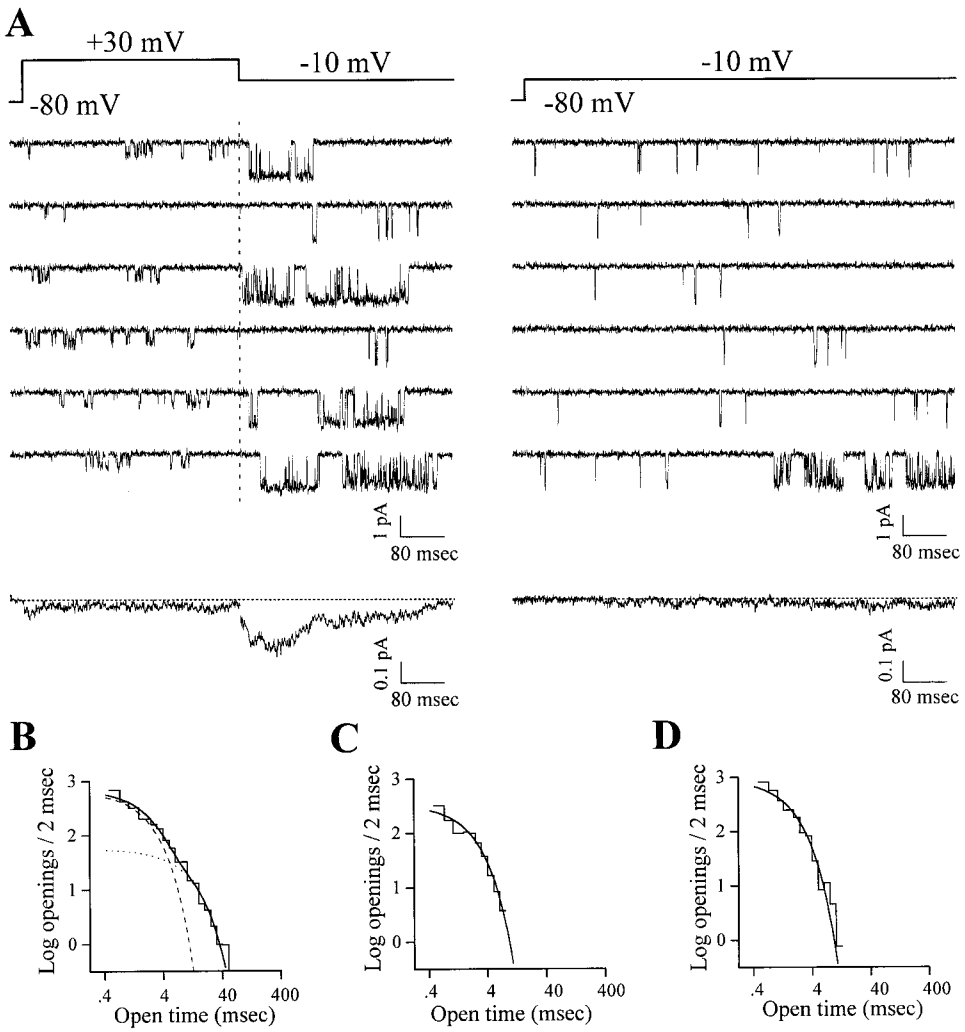

FIGURE 8. Positive depolarizations drive anomalous L-type channels from a short-opening gating mode into a long-opening mode. Single-channel recordings from a single-channel excised patch with one anomalous L-type channel, in the presence of 1 μM (+)-(S)-202-791 in the bath. Control (800-ms long) depolarizations to −10 mV were alternated with a voltage protocol in which the depolarization to −10 mV was preceded by a prepulse to +30 mV for 400 ms. The two protocols were separated by 4 s at −80 mV. Cell B48L. (A) Representative current traces showing the single channel activity at +30 mV during the prepulse and at −10 mV after the prepulse (left), and at −10 mV in control depolarizations (right). Below the traces, the corresponding ensemble average currents are shown (left, n = 112; right, n = 146). The decay of the average current at −10 mV after the prepulse towards the control value was best fit by an exponential with a time constant of 152 ms, while its rising phase was best fit by an exponential with time constant of 14 ms. (B) Log–log plot of the open time distribution at −10 mV after the prepulse (n = 79). Best fit required two exponential components with time constants of 1.7 and 9.1 ms and relative areas of 67 and 33%, respectively. (C) Log–log plot of the open time distribution at −10 mV after the prepulse in traces with $P_o < 0.1$ (n = 50). Best fit required a single exponential with a time constant of 1.6 ms. (D) Log–log plot of the open time distributions at −10 mV in control depolarizations (n = 98), after exclusion of four traces with the mode shift ($P_o > 0.1$, see last representative control trace in A). Best fit required one exponential with time constant of 1.4 ms.

the time constant obtained from the best fit of the open time histogram of control traces (excluding the four traces with the mode shift having $P_o > 0.1$).

The average current at −10 mV after the predepolarization shows a clear rising phase, and after reaching a maximum value, slowly decays towards the control value. On average, the time constant of decay was 177 ± 28 ms (n = 4). The decay of the potentiated current should mainly reflect the kinetics of return of the channel from the long-opening mode to the short-opening mode prevailing in control. The slower decay of the average current at −10 mV with respect to that at −60 mV after the depolarization (46 ± 2 ms, n = 6, see Fig. 5) is consistent with the voltage dependence of k_b, whereby k_b decreases with increasing voltage (Pietrobon and Hess, 1990; Forti and Pietrobon, 1993). The rising phase of the current at −10 mV is clearly slower than the rising phase of the current at −60 mV after a similar prepulse (see Fig. 5), indicating that the rate of reopening from the closed states accessed during the depolarization (C_b and C^*_b) increases with more negative repolarization voltages. On average, the time constant of the rising phase increased from 2.6 ± 0.3 ms (n = 6) at −60 mV to 11 ± 2 ms (n = 4) at −10 mV. This finding is consistent with and supports the voltage dependence of the rate constants of exit from the closed states C_b and C^*_b in the model in Fig. 6, whereby β and β* decrease with increasing voltage. Consistent with this voltage dependence is also the peculiar lengthening of the closed times with increasing voltage of the depolarization (see Figs. 3 B and 10 B).

The two open time constants, obtained from the biexponential open time histogram at −10 mV were both smaller than those obtained for the reopenings at

−60 mV after a similar depolarization (compare Figs. 8 and 5). On the other hand, the open time constants at both −10 and −60 mV were larger than those obtained from the histogram of open times during the preceding depolarization (Fig. 3). In the voltage range −60 to +40 mV, the open time constants decreased as shown in Fig. 9 A. This anomalous voltage dependence of the open times supports the existence, within each mode, of a closed state outside the activation pathway to which the open state is connected through a transition whose rate constant increases with increasing voltage. Accordingly, in Fig. 6, the open states within each mode (O, O*) are connected to a closed state outside the activation pathway (C_b, C^*_b), and the rate constants α, α^* for entry into these closed states increase with increasing voltage. Our interpretation that the fast and slow components in the open-time histograms reflect sojourns in the open states of modes 1 and 2, respectively, is further supported by the finding that, as already pointed out, the contribution of the slow exponential component in the open time histograms increases with increasing depolarization voltage, with a symmetrical decrease of the fast component (Fig. 3 A, right).

At voltages higher than +20 mV, the two open time constants become similar (Figs. 3 A and 9 A). At these positive voltages, the anomalous L-type channel in mode 2 opens only for brief times, thus explaining the absence of bursts of activity with long openings during depolarizations effective in inducing the change to the long-opening mode as seen on repolarization (Fig. 8 A). One predicts that the potentiation of the anomalous L-type current by positive depolarizations should decrease with increasing repolarization voltage and there should be no potentiation of the current at repolarization voltages higher than +20 mV. Fig. 9 B shows that, in a single channel patch, the unitary activity of an anomalous L-type channel at +20 mV after a predepolarization to +40 mV for 400 ms was hardly distinguishable from that in control depolarizations at +20 mV. As a result, the same depolarization that produced a ro-

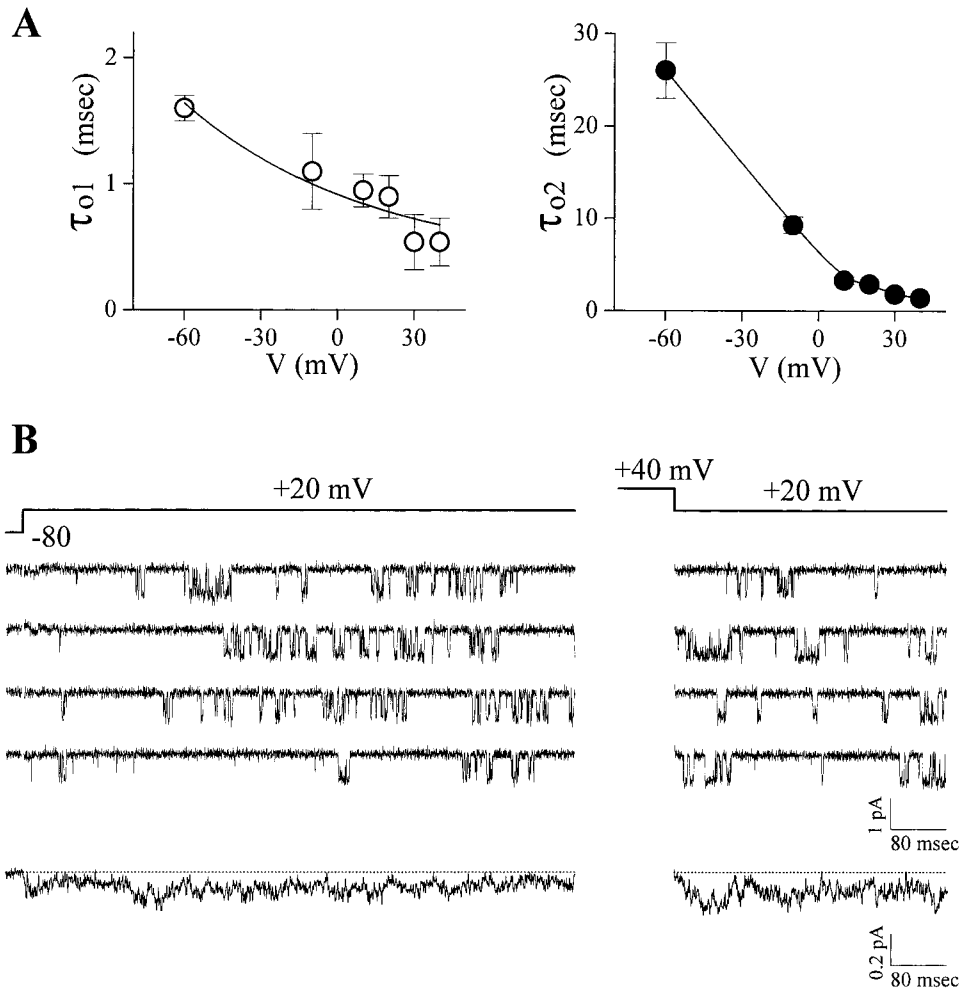

FIGURE 9. The open times of anomalous L-type channels shorten with increasing voltage and become similar in modes 1 and 2 at V > +20 mV. (A) Voltage dependence of the two time constants, τ_{o1} and τ_{o2}, best fitting the open time histograms of anomalous L-type channels. The data points are averages from three (−10, +10, +30, +40 mV), five (+20 mV), and six (−60 mV) patches, containing either one or two anomalous L-type channels (in the latter case only traces without overlappings were considered). The time constants at −10 and −60 mV were obtained from open time histograms of activity following a 400-ms-long depolarization at +30/+40 mV. The time constants at +10 to +40 mV were obtained from the activity during depolarizations at the different voltages. (B) Cell-attached single channel recordings from a patch containing one anomalous L-type channel, in the presence of 1 μM (+)-(S)-202-791 in the bath. Control (800-ms-long) depolarizations to +20 mV were alternated with a voltage protocol in which the depolarization to +20 mV was preceded by a prepulse to +40 mV for 400 ms. The two protocols were separated by 4 s at −80 mV. Representative current traces showing the single channel activity at +20 mV in control depolarizations (left) and at the same voltage following the prepulse (right) are displayed together with the corresponding ensemble average currents (left, $n = 38$; right, $n = 28$). Cell B49A.

bust potentiation of the average current at −10 mV (Fig. 8), hardly potentiated the current at +20 mV.

Although Forti and Pietrobon (1993) did not speculate on the nature of C_b and C^*_b, these states might correspond to either particular conformations of the channel or to open-pore blocked states, as proposed by Slesinger and Lansman (1996). In the latter case, α, β and α*, β* would be the rate constants of voltage-dependent block and unblock of the channel in the short- and long-opening modes, respectively, and their voltage dependence would be consistent with block by a positively charged cytoplasmic particle (Slesinger and Lansman, 1996). However, the result shown in Fig. 10 excludes any diffusible ion as the blocking particle. After excision in the K-gluconate/EGTA solution without divalents, the anomalous gating can persist unaltered for 40 min. Indeed, the data shown in Figs. 4 and 8 were derived after excision of the patch. The voltage-dependent induction of the long-opening mode in the inside-out patch in Fig. 8 shows that a diffusible cytosolic factor is not necessary for voltage-dependent potentiation of anomalous L-type channels.

discussion

In this study, we have shown that embryonic rat spinal motoneurons express anomalous L-type calcium channels, which reopen upon repolarization to resting potentials, displaying both short and long reopenings. The probability of reopening increases with increasing voltage of the preceding depolarization without any apparent correlation with inactivation during the depolarization. The probability of long with respect to short reopenings increases with increasing length of the depolarization, with little change in the total number of reopenings and in their delay. With less negative repolarization voltages, the delay increases, while the mean duration of both short and long reopenings decreases, remaining longer than that of the openings during the preceding depolarization. Open times decrease with increasing voltage in the range −60 to +40 mV, while closed times tend to increase with voltage at $V > 20$ mV. The open probability during depolarizing pulses is low at all voltages and has an anomalous bell-shaped voltage dependence.

We have provided evidence that the two open states, leading to short and long reopenings, correspond to two gating modes of the channel, whose relative probability depends on voltage. Since the sojourn of the channel in both open states decreases with increasing voltage, the two open states must be connected to a closed state outside the activation pathway with a voltage-dependent transition whose rate constant increases with increasing voltage. The anomalous voltage dependence of the closed times suggests that the rate constant of reopening from this closed state decreases with increasing voltage. This voltage dependence leads to reopening of the channel upon repolarization and predicts a faster rate of reopening at more negative repolarization voltages, as found. According to our data,

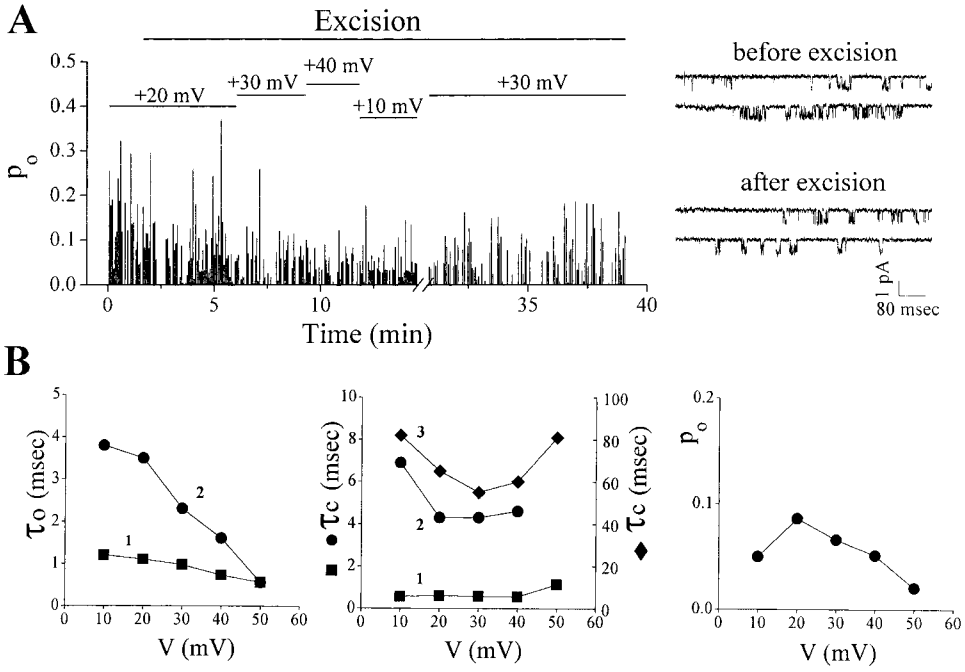

FIGURE 10. The anomalous gating persists after patch excision. Single channel recordings from a patch containing one anomalous L-type channel, in the presence of 1 μM (+)-(S)-202-791 in the bath. After 3 min of recording in the cell-attached configuration, the patch was excised in the inside out configuration; i.e., with the internal side facing the K-gluconate-EGTA bath solution. Cell B48L. (A) Representative current traces at +20 mV before and after excision are shown together with a diary plot displaying the open probability of the channel in successive depolarizations as a function of time during the recording. Depolarizations were 724- or 800-ms long and were separated by 4 s at −80 mV. During the recording, the test pulse voltage changed as indicated above the thin horizontal lines. The time after excision is indicated by the thick horizontal line. (B) Voltage dependence of the open probability and of the time constants of the exponential components best fitting open (τ_{o1} and τ_{o2}) and closed (τ_{c1}, τ_{c2} and τ_{c3}) time distributions after patch excision are shown.

positive voltages favor both the transition from a short-opening gating mode (mode 1) to a long-opening mode (mode 2), and the occupancy of a closed state within each mode from which the channel reopens on repolarization, displaying short reopenings when it reopens from the closed state of mode 1 and long reopenings when it reopens from the closed state of mode 2 (Fig. 6, C_b and C^*_b) (Forti and Pietrobon, 1993). The voltage dependence of the probability of reopenings reflects the voltage dependence of the occupancy of the closed states from which the channel reopens, while the relative probability of long with respect to short reopenings reflects the voltage dependence of the equilibrium between modes.

The properties of the first latency distribution of reopenings of anomalous L-type channels of mouse cerebellar granule cells, measured by Slesinger and Lansman (1996) as a function of repolarization voltage, are consistent with our conclusions. To explain their data, Slesinger and Lansman (1996) assumed the existence of a positively charged cytoplasmic blocking particle that may reversibly block the pore during the depolarization and be released upon repolarization at negative membrane potentials. According to this interpretation, C_b and C^*_b would correspond to open-pore blocked states. Our finding that the anomalous gating persists after excision of the patch in divalent-free solution rules out block by a diffusible ion. It does not rule out block by a membrane-bound particle. The abrupt switch from the anomalous gating to the cardiac-type gating, observed by Forti and Pietrobon (1993) in one single channel patch, tends to exclude part of the channel as the blocking particle. An alternative interpretation, consistent with all the available data, is that C_b and C^*_b represent conformational states of the channel and that voltage-dependent pore block is not involved in anomalous gating.

Our data, both in motoneurons and cerebellar granule cells, do not show any apparent inactivation of single anomalous L-type channels during depolarizations effective in inducing reopenings, even though the kinetic scheme in Fig. 6 is clearly compatible with inactivation and actually might seem to be inconsistent with lack of inactivation. Simulations performed using the model in Fig. 6 show that, depending on the rate constants of the transitions between the states within each mode, the model can generate both noninactivating and inactivating currents during depolarizations effective in inducing reopenings (not shown). The extent of inactivation depends crucially on the ratio between forward and backward rate constants, and increases with increasing ratios above a certain value. Thus, the model predicts that macroscopic inactivation should become apparent at sufficiently high voltages. The fact that it was not apparent from our single channel ensemble averages in the range from +10 to +40 mV may signify that these voltages were not sufficiently high. Alternatively, a small extent of inactivation at high voltages might have been missed, due to the stochastic behavior in the records.

Voltage-dependent potentiation is an interesting property shared by the different L-type channels described so far. This name refers to the ability of earlier depolarization to transiently increase macroscopic L-type current. In different cells, different voltage dependence, different time course, and different duration of voltage-dependent potentiation of L-type channels have been reported, reflecting different L-type channels and/or different modulatory mechanisms (Fenwick et al., 1982; Hoshi et al., 1984; Lee, 1987; Pietrobon and Hess, 1990; Artalejo et al., 1991, 1992; Forti and Pietrobon, 1993; Nakayama and Brading, 1993; Sculptoreanu et al., 1993a,b, 1995; Bourinet et al., 1994; Johnson et al., 1994; Kleppisch et al., 1994; Fleig and Penner, 1996; Kavalali and Plummer, 1996; Parri and Lansman, 1996; Cloues et al., 1997). The progressive shift towards a long-opening mode induced by increasing voltage can explain the voltage-dependent potentiation of L-type channels of cardiac (Pietrobon and Hess, 1990) and smooth muscle cells (Kleppisch et al., 1994), as well as that of cardiac-type neuronal L-type channels (Bourinet et al., 1994; Kavalali and Plummer, 1996, and our unpublished observations). We have shown here and in our previous work (Forti and Pietrobon, 1993) that a voltage-dependent change in gating mode is also at the basis of voltage-dependent potentiation of anomalous L-type channels.

The closed states giving rise to the anomalous gating confer to the voltage-dependent potentiation of anomalous L-type channels two specific properties. The transient increase of anomalous L-type current following a depolarization is delayed, and falls with increasing repolarization voltage to become almost zero at +20 mV, where the open probability in the two modes becomes similar. In similar experimental conditions, potentiation of cardiac L-type channels (Pietrobon and Hess, 1990) and brain α_{1C} (Bourinet et al., 1994) is still observed at +20 mV, where the open probability of the two modes is still quite different. Anomalous L-type channels differ from cardiac-type channels also in the voltage range controlling the mode change, which is shifted to lower voltages for anomalous L-type channels (Pietrobon and Hess, 1990; Kavalali and Plummer, 1996). Furthermore, the potentiation lasts longer for anomalous L-type channels with respect to cardiac channels (see Figure 4 of Forti and Pietrobon, 1993).

An important specific property of anomalous L-type channels is that even very short or small depolarizations, insufficient to significantly shift the channels towards the long-opening mode, can induce short re-

openings and thus transiently increase, for a brief time, the current upon repolarization. By delaying channel opening at resting potential, where the driving force is larger, the closed/blocked state from which anomalous L-type channels reopen provides a mechanism to maximize calcium influx after a transient membrane depolarization such as an action potential. With increasing duration and amplitude of the depolarization, the relative contribution of long reopenings, due to the mode shift, increases, leading to a potentiated and longer lasting transient increase of the current upon repolarization. The anomalous gating warrants maximal potentiation at resting potentials. One can predict that a presynaptic train of action potentials at high frequency may lead to a progressive increase of calcium influx through presynaptic anomalous L-type channels during the train, and/or may generate a large surge of calcium influx through postsynaptic anomalous L-type channels at the end of the train. Reopenings of L-type channels after single action potentials, with increasing open times at more negative repolarization voltages, and a progressive shift of the same channels to a long-opening gating mode during trains of action potentials have been observed in sensory neurons (Ferroni et al., 1996). Reopenings of calcium channels induced by single back-propagating action potentials have been observed also in dendrites of hippocampal cells (Magee and Johnston, 1995). Most likely, anomalous L-type channels were involved in both cases. Kavalali and Plummer (1994, 1996) and Kavalali et al. (1997) have characterized L-type channels in hippocampal neurons with biophysical properties quite similar to those of anomalous L-type channels of cerebellar granule cells and motoneurons. The similarities include single channel current and conductance, low open probability, mean open times at +20 mV shorter than at −30 mV, potentiation after modest depolarizations (LVP) and lack of potentiation at repolarization voltages higher than +20 mV, slower decay of the potentiated current than that of cardiac L-type channels, and persistent activity in excised patches.

Given their presence in cerebellar, hippocampal, sensory, and motor neurons, L-type channels with anomalous gating are probably widely expressed in the nervous system, while they are absent from cardiac and pituitary endocrine cells (our unpublished observations). The predicted capability of anomalous L-type channels to produce a delayed influx of calcium at resting potentials after previous neuronal electrical activity, whose extent depends on the duration and strength of such activity, makes them particularly suited to play a critical role in coupling transient neuronal activity with long-term changes in nervous system development and function. Indeed, several of these changes have been found to be specifically inhibited by dihydropyridine drugs (see INTRODUCTION). Calcium entry through anomalous L-type channels might play an important role also in neurotoxic pathogenesis, since these channels are probably still active under conditions of metabolic stress such as hypoxia, which would favor the voltage-dependent change in gating mode leading to potentiation of calcium influx. In addition, anomalous L-type channels may play a role in neuronal deterioration during aging (Thibault and Landfield, 1996).

The molecular basis for the anomalous L-type channel is unknown. Its absence in pituitary endocrine cells, which express the α_{1D} subunit in large amounts (Fomina et al., 1996), and, on the other hand, its abundance in rat cerebellar granule cells in primary culture, where the α_{1D} subunit is either not expressed or expressed in small amounts (Schramm et al., 1999), suggest that, most likely, the pore-forming subunit of anomalous L-type channels is not α_{1D}. Since the α_{1C} subunit was detected as a major transcript in rat cerebellar granule cells in primary culture using degenerated oligonucleotide primer pairs under highly stringent conditions, and no new α_1-related sequences were amplified under the same conditions (Schramm et al., 1999), it appears likely that the anomalous L-type channel is related to the α_{1C} subunit. It remains to be established whether the anomalous behavior arises from an unknown splice variant of the α_{1C} subunit, from a particular subunit composition, or from an unknown type of modulation.

We thank Dr. C.E. Henderson for providing the IgG-192 hybridoma and Dr. M. Cantini for providing the muscle-conditioned medium.

The financial support of Telethon-Italy to D. Pietrobon (grant 720) and to B. Hivert is gratefully acknowledged. This work was also partially supported by a grant from the Regione del Veneto (Giunta Regionale Ricerca Sanitaria Finalizzata-Venezia-Italia).

Original version received 19 January 1999 and accepted version received 25 March 1999.

references

Aniksztejn, L., and Y. Ben-Ari. 1991. Novel form of long-term potentiation produced by a K^+ channel blocker in the hippocampus. *Nature.* 349:67–69.

Artalejo, C.R., D.J. Mogul, R.L. Perlman, and A.P. Fox. 1991. Three types of bovine chromaffin cell Ca^{2+} channels: facilitation increases the opening probability of a 27 pS channel. *J. Physiol.* 444: 213–240.

Artalejo, C.R., S. Rossie, R.L. Perlman, and A.P. Fox. 1992. Voltage-dependent phosphorylation may recruit Ca^{2+} current facilitation in chromaffin cells. *Nature.* 358:63–66.

Bading, H., D.D. Ginty, and M.E. Greenberg. 1993. Regulation of gene expression in hippocampal neurons by distinct calcium signaling pathways. *Science.* 260:181–186.

Bolshakov, V.Y., and S.A. Siegelbaum. 1994. Postsynaptic induction and presynaptic expression of hippocampal long-term depression. *Science.* 264:1148–1152.

Bourinet, E., P. Charnet, W.J. Tomlinson, A. Stea, T.P. Snutch, and J. Nargeot. 1994. Voltage-dependent facilitation of a neuronal α_{1C} L-type calcium channel. *EMBO (Eur. Mol. Biol. Organ.) J.* 13: 5032–5039.

Brosenitsch, T.A., D. Salgado-Commissariat, D.L. Kunze, and D.M. Katz. 1998. A role for L-type calcium channels in developmental regulation of transmitter phenotype in primary sensory neurons. *J. Neurosci.* 18:1047–1055.

Camu, W., E. Bloch-Gallego, and C.E. Henderson. 1993. Purification of spinal motoneurons from chicken and rat embryos by immunopanning. *Neuroprotocols.* 2:191–199.

Cloues, R.K., S.J. Tavalin, and N.V. Marrion. 1997. b-Adrenergic stimulation selectively inhibits long-lasting L-type calcium channel facilitation in hippocampal pyramidal neurons. *J. Neurosci.* 17:6493–6503.

Collins, F., M.F. Schmidt, P.B. Guthrie, and S.B. Kater. 1991. Sustained increase in intracellular calcium promotes neuronal survival. *J. Neurosci.* 11:2582–2587.

Colquhoun, D., and F.J. Sigworth. 1983. Fitting and statistical analysis of single-channel records. *In* Single Channel Recordings. B. Sakmann and E. Neher, editors. Plenum Publishing Corp., New York. 191–264.

Deisseroth, K., K.E. Heist, and R.W. Tsien. 1998. Translocation of calmodulin to the nucleus supports CREB phosphorylation in hippocampal neurons. *Nature.* 392:198–202.

Demo, S.D., and G. Yellen. 1991. The inactivation gate of the *Shaker* K^+ channel behaves like an open-channel blocker. *Neuron.* 7:743–753.

Fenwick, E.M., A. Marty, and E. Neher. 1982. Sodium and calcium channels in bovine chromaffin cells. *J. Physiol.* 331:599–635.

Ferroni, A., A. Galli, and M. Mazzanti. 1996. Functional role of low-voltage activated dihydropyridine-sensitive Ca channels during the action potential in adult rat sensory neurons. *Pflügers Arch.* 431:954–963.

Finkbeiner, S., and M.E. Greenberg. 1996. Ca^{2+}-dependent routes to Ras: mechanisms for neuronal survival, differentiation, and plasticity? *Neuron.* 16:233–236.

Fisher, R.E., R. Gray, and D. Johnston. 1990. Properties and distribution of single voltage-gated calcium channels in adult hippocampal neurons. *J. Neurophysiol.* 64:91–104.

Fleig, A., and R. Penner. 1996. Silent calcium channels generate excessive tail currents and facilitation of calcium currents in rat skeletal myoballs. *J. Physiol.* 494:141–153.

Fomina, A.F., E.S. Levitan, and K. Takimoto. 1996. Dexamethasone rapidly increases calcium channel subunit messenger RNA expression and high voltage-activated calcium current in clonal pituitary cells. *Neuroscience.* 72:857–862.

Forti, L., and D. Pietrobon. 1993. Functional diversity of L-type calcium channels in rat cerebellar neurons. *Neuron.* 10:437–450.

Galli, C., O. Meucci, A. Scorziello, T.M. Werge, P. Calissano, and G. Schettini. 1995. Apoptosis in cerebellar granule cells is blocked by high KCl, forskolin, and IGF-1 through distinct mechanisms of action: the involvement of intracellular calcium and RNA synthesis. *J. Neurosci.* 15:1172–1179.

Ghosh, A., J. Carnahan, and M.E. Greenberg. 1994. Requirement for BDNF in activity-dependent survival of cortical neurons. *Science.* 263:1618–1623.

Grover, L.M., and T.J. Teyler. 1990. Two components of long-term potentiation induced by different patterns of afferent activation. *Nature.* 347:477–479.

Hamill, O.P., A. Marty, E. Neher, B. Sakmann, and F.J. Sigworth. 1981. Improved patch-clamp techniques for high-resolution current recording from cells and cell-free membrane patches. *Pflügers Arch.* 391:85–100.

Hivert, B., S. Bouhanna, S. Dochot, W. Camu, G. Dayanithi, C.E. Henderson, and J. Valmer. 1995. Embryonic rat motoneurons express a functional P-type voltage-dependent calcium channel. *Int. J. Dev. Neurosci.* 13:429–436.

Hivert, B., and D. Pietrobon. 1995. Calcium channels of embryonic rat motoneurons. *Soc. Neurosci.* 21:1578. (Abstr.)

Hivert, B., and D. Pietrobon. 1997. Anomalous L-type calcium channels of rat spinal motoneurons. *Biophys. J.* 72:A22. (Abstr.)

Hoshi, T., J. Rothlein, and R.J. Smith. 1984. Facilitation of Ca^{2+} channel currents in bovine adrenal chromaffin cells. *Proc. Natl. Acad. Sci. USA.* 81:5871–5875.

Johnson, B.D., T. Scheuer, and W.A. Catterall. 1994. Voltage-dependent potentiation of L-type Ca^{2+} channels in skeletal muscle cells requires anchored cAMP-dependent protein kinase. *Proc. Natl. Acad. Sci. USA.* 91:11492–11496.

Johnston, D., S. Williams, D. Jaffe, and R. Gray. 1992. NMDA-receptor independent long-term potentiation. *Annu. Rev. Physiol.* 54: 489–505.

Kavalali, E.T., K.S. Hwang, and M.R. Plummer. 1997. cAMP-dependent enhancement of dihydropyridine-sensitive calcium channel availability in hippocampal neurons. *J. Neurosci.* 17:5334–5348.

Kavalali, E.T., and M.R. Plummer. 1994. Selective potentiation of a novel calcium channel in rat hippocampal neurones. *J. Physiol.* 480:475–484.

Kavalali, E.T., and M.R. Plummer. 1996. Multiple voltage-dependent mechanisms potentiate calcium channel activity in hippocampal neurons. *J. Neurosci.* 16:1072–1082.

Kirsch, J., and H. Betz. 1998. Glycine-receptor activation is required for receptor clustering in spinal neurons. *Nature.* 392:717–720.

Kleppisch, T., K. Pedersen, C. Strübing, E. Bosse-Doenecke, V. Flockerzi, F. Hofmann, and J. Hescheler. 1994. Double-pulse facilitation of smooth muscle a_1 subunit Ca^{2+} channels expressed in CHO cells. *EMBO (Eur. Mol. Biol. Organ.) J.* 13:2502–2507.

Kullmann, D.M., D.J. Perkel, T. Manabe, and R.A. Nicoll. 1992. Ca^{2+} entry via postsynaptic voltage-sensitive Ca^{2+} channels can transiently potentiate excitatory synaptic transmission in the hippocampus. *Neuron.* 9:1175–1183.

Lee, K. 1987. Potentiation of calcium channel currents of internally perfused mammalian heart cells by repetitive depolarization. *Proc. Natl. Acad. Sci. USA.* 84:3941–3945.

Magee, J.C., and D. Johnston. 1995. Synaptic activation of voltage-gated channels in the dendrites of hippocampal pyramidal neurons. *Science.* 268:301–307.

Magnelli, V., P. Baldelli, and E. Carbone. 1998. Antagonists-resistant calcium currents in rat embryo motoneurons. *Eur. J. Neurosci.* 10:1810–1825.

McManus, O.B., A.L. Blatz, and K.L. Magleby. 1987. Sampling, log binning, fitting and plotting durations of open and shut intervals from single channels and the effect of noise. *Pflügers Arch.* 410: 530–553.

Murphy, T.H., P.F. Worley, and J.M. Baraban. 1991. L-type voltage-sensitive calcium channels mediate synaptic activation of immediate early genes. *Neuron.* 7:625–635.

Mynlieff, M., and K.G. Beam. 1992. Characterization of voltage-dependent calcium currents in mouse motoneurons. *J. Neurophysiol.* 68:85–92.

Nakayama, S., and A.F. Brading. 1993. Evidence for multiple open states of the Ca^{2+} channels in smooth muscle cells isolated from the guinea-pig detrusor. *J. Physiol.* 471:87–105.

Neher, E. 1992. Correction for liquid junction potentials in patch

clamp experiments. *Methods Enzymol.* 207:123–131.

Parri, H.R., and J.B. Lansman. 1996. Multiple components of Ca^{2+} channel facilitation in cerebellar granule cells: expression of facilitation during development in culture. *J. Neurosci.* 16:4890–4902.

Pietrobon, D., and P. Hess. 1990. Novel mechanism of voltage-dependent gating in L-type calcium channels. *Nature.* 346:651–655.

Rao, C.R. 1973. Linear statistical inference and its applications. 2nd edition. John Wiley & Sons, New York. 400 pp.

Schramm, M., R. Vajna, A. Pereverzev, A. Tottene, U. Klockner, D. Pietrobon, J. Hescheler, and T. Schneider. 1999. Isoforms of alpha1E voltage-gated calcium channels in rat cerebellar granule cells. Detection of major calcium channel alpha1-transcripts by reverse transcription-polymerase chain reaction. *Neuroscience.* In press.

Sculptoreanu, A., A. Figourov, and W.C. De Groat. 1995. Voltage-dependent potentiation of neuronal L-type calcium channels due to state-dependent phosphorylation. *Am. J. Physiol.* 269: C725–C732.

Sculptoreanu, A., E. Rotman, M. Takahashi, T. Scheuer, and W.A. Catterall. 1993a. Voltage-dependent potentiation of the activity of cardiac L-type calcium channel alpha 1 subunits due to phosphorylation by cAMP-dependent protein kinase. *Proc. Natl. Acad. Sci. USA.* 90:10135–10139.

Sculptoreanu, A., T. Scheuer, and W.A. Catterall. 1993b. Voltage-dependent potentiation of L-type Ca^{2+} channels due to phosphorylation by cAMP-dependent protein kinase. *Nature.* 364:240–243.

Shitaka, Y., N. Matsuki, H. Saito, and H. Katsuki. 1996. Basic fibroblast growth factor increases functional L-type Ca^{2+} channels in fetal rat hippocampal neurons: implications for neurite morphogenesis in vitro. *J. Neurosci.* 16:6476–6489.

Sigworth, F.J., and S.M. Sine. 1987. Data transformation for improved display and fitting of single-channel dwell time histograms. *Biophys. J.* 52:1047–1054.

Slesinger, P.A., and J.B. Lansman. 1991. Reopening of Ca^{2+} channels in mouse cerebellar neurons at resting membrane potentials during recovery from inactivation. *Neuron.* 7:755–762.

Slesinger, P.A., and J.B. Lansman. 1996. Reopening of single L-type Ca^{2+} channels in mouse cerebellar granule cells: dependence on voltage and ion concentration. *J. Physiol.* 491:335–345.

Snutch, T.P., W.J. Tomlinson, J.P. Leonard, and M.M. Gilbert. 1991. Distinct calcium channels are generated by alternative splicing and are differentially expressed in the mammalian CNS. *Neuron.* 7:45–57.

Soldatov, N.M., A. Bouron, and H. Reuter. 1995. Different voltage-dependent inhibition by dihydropyridines of human Ca^{2+} channel splice variants. *J. Biol. Chem.* 270:10540–10543.

Thibault, O., and P.W. Landfield. 1996. Increase in single L-type calcium channels in hippocampal neurons during aging. *Science.* 272:1017–1020.

Thibault, O., N.M. Porter, and P.W. Landfield. 1993. Low Ba^{2+} and Ca^{2+} induce a sustained high probability of repolarization openings of L-type Ca^{2+} channels in hippocampal neurons: physiological implications. *Proc. Natl. Acad. Sci. USA.* 90:11792–11796.

Umemiya, M., and A.J. Berger. 1994. Properties and function of low- and high-voltage-activated Ca^{2+} channels in hypoglossal motoneurons. *J. Neurosci.* 14:5652–5660.

Umemiya, M., and A.J. Berger. 1995. Single-channel properties of four calcium channel types in rat motoneurons. *J. Neurosci.* 15: 2218–2224.

Williams, M.E., D.H. Feldman, A.F. McCue, R. Brenner, G. Velicelebi, S.B. Ellis, and M.M. Harpold. 1992. Structure and functional expression of α_1, α_2, and β subunits of a novel human neuronal calcium channel subtype. *Neuron.* 8:71–84.